Milutin G. Jovanović

University of Northumbria at Newcastle. School of Computing, Engineering and Information Sciences. Newcastle upon Tyne NE1 8ST, UK
Fax: +44-191-2273598;
milutin.jovanovic@unn.ac.uk

J. Electrical Systems 2-4 (2006): 208-225

Regular paper

A Comparative Study of Control Strategies for Performance Optimisation of Brushless Doubly-Fed Reluctance Machines

The brushless doubly-fed machine (BDFM) allows the use of a partially rated inverter and represents an attractive cost-effective candidate for variable speed applications with limited speed ranges. In its induction machine form (BDFIM), the BDFM has significant rotor losses and poor efficiency due to the cage rotor design which makes the machine dynamic models heavily parameter dependent and the resulting controller configuration complicated and difficult to implement. A reluctance version of the BDFM, the brushless doubly-fed reluctance machine (BDFRM), ideally has no rotor losses, and therefore offers the prospect for higher efficiency and simpler control compared to the BDFIM. A detailed study of this interesting and emerging machine is very important to gain a thorough understanding of its unusual operation, control aspects and compromises between optimal performance and the size of the inverter and the machine. This paper will attempt to address these issues specifically concentrating on developing conditions for various control properties of the machine such as maximum power factor, maximum torque per inverter ampere and minimum copper losses, as well as analysing the associated trade-offs.

Keywords: Double Fed Induction Generator, Variable Speed, Isolated Site Voltage Supplying, Stator Voltage Constant Key-Parameters, Scalar Control, Modeling.

1. INTRODUCTION

With the advent of power electronics and microprocessor technology, it has become possible to better control and utilise Brushless Doubly-Fed Machines (BDFMs) to the point where they have started to be considered as a potential alternative to the existing drive solutions in a variety of low to medium performance industrial applications. The two main reasons have largely contributed to this growing interest in the machines: (1) their slip power recovery operating nature allowing the deployment of a partially-rated converter, and (2) the absence of brush gear and consequent reliable, virtually maintenance-free operation.

The fact that the feeding converter only has to handle the slip power implies significant cost savings (up to 30%) compared to systems with fully rated inverters [1]. This is particularly true in larger drives with limited variable speed capability (e.g. pumps [2, 3], wind turbines [3-5], heating, ventilation and air-conditioning etc.) where, despite the falling market prices, the power electronic hardware still represents a major portion of the total cost. A cost penalty would incurred for the machine but this would be more than offset by the reduction in the converter cost (for a typical speed range of 2:1, its real power rating can be limited to about 25% of the machine's [3, 6, 7]). Other benefits of using the smaller inverter include the improved supply quality and the lower filtering requirements, as less harmonics are injected into the grid.

The reliability of brushless design and low maintenance make the BDFMs preferable to a conventional Doubly Excited Wound Rotor Induction Machine (DEWRIM), for example, in off-shore wind power applications where these two features become crucially important due to the cost implications [8].

The BDFM shares all the advantages of doubly fed machines over singly excited counterparts - operational mode flexibility, the greater control freedom, and the possibility of sub-synchronous and super-synchronous speed operation in both motoring and generating regimes. It can operate as a standard or doubly excited induction machine, and as a fixed or adjustable speed synchronous turbo-machine [5]. The latter operating mode means that high speed, field weakened traction applications [9], as well as high frequency generators [10] are feasible. In the former applications, the ability of the BDFM to function as an induction machine in case of the inverter failure is an important "fail-safe" measure. From a control viewpoint, one merit of the machine is that one can not only control its real power, but also the power factor, efficiency or any other performance parameter of interest.

Replacing a special cage rotor [11] with a cageless reluctance type (Fig. 1), which can be similar to that of a modern synchronous reluctance machine (Syncrel) [6, 12], would further improve the machine's overall performance (this is known as the Brushless Doubly-Fed Reluctance Machine, or BDFRM), and especially with rotors having higher saliency ratios [6][1]. The possibility of using commercially available Syncrel rotors would also reduce the manufacturing cost of the machine. Apart from being less expensive, the BDFRM should be more efficient [14], more mechanically robust, and much easier to model/control than the BDFIM [15, 16]. In contrast to the latter, field-oriented (vector) control of the primary reactive power and electromagnetic torque is inherently decoupled in the BDFRM (so is with the DEWRIM) [16]. Furthermore, the BDFRM does not suffer from stability problems inherent with the BDFIM around the zero-torque operating point at synchronous speed of the grid-connected winding field [17]. This means that, unlike the BDFIM, the BDFRM can be operated stably over the entire speed range down to standstill. For these reasons, this paper will limit its scope to the BDFRM as more promising of the two distinct BDFM types.

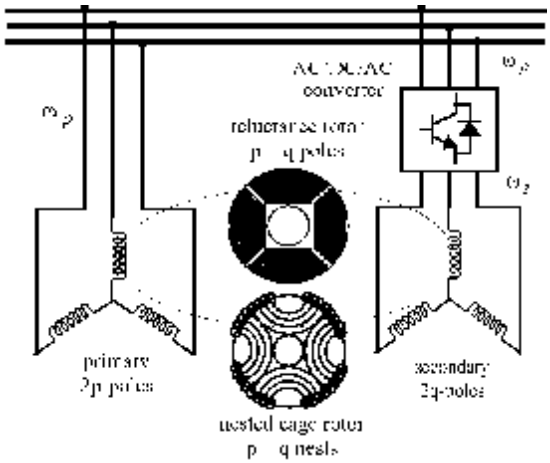

Fig. 1. Structural diagram of the 6/2-pole BDFM with an axially-laminated rotor (top) and nested cage rotor (bottom).

As can be seen from Fig. 1, the machine has two individual stator windings (the grid-connected primary or `power' winding, and the inverter-fed secondary or `control' winding) of different pole numbers and applied frequencies, and a rotor having half the total number of stator poles (or nests with the BDFIM) to provide magnetic coupling between the windings and torque production from the machine. Note that this design peculiarity means that the rotor may have an odd pole number (i.e. 3 for 4/2-pole stator windings [4, 18]) as opposed to a conventional machine where this is always even. Yet, the BDFRM prototypes

[1]Recent finite-element modelling studies have shown that with an appropriate rotor design even performance competitive to traditional induction machines can be achieved [13].

with a 6/2-pole stator and a 4-pole rotor have been almost exclusively reported in the literature.

One of the BDFRM's main attributes is its power factor control ability. The power factor in the inverter-fed (secondary) winding is relevant to the inverter size, but is irrelevant to the outside utility network (since the inverter effectively isolates the secondary from the mains supply). However the power factor of the machine's grid connected (primary) winding is of great importance (especially in weak networks) in the light of new regulations coming into force around the world on this issue. In order to minimise the total current loading (hence losses) for a given real power demand, it is therefore desirable to keep the primary power factor near or at unity. One can also generate VARs into the power grid to provide voltage support, but the price to pay is the need for a bi-directional (dual bridge) power converter [19] of higher rating.

The fundamental space-vector theory and dynamic models for the BDFRM have already been established in [7, 19, 20], and comparisons of theoretical performance limitations with the closely-related Syncrel have been made in [6]. The `traditional' control methods commonly encountered in the open literature on other, more conventional machines have been applied to the BDFRM as well - a scalar control algorithm has been proposed in [3], vector control principles have been considered in [4, 16, 21], and even direct torque control (DTC) schemes have been developed [22] and experimentally verified [23]. The importance and main contribution of the work to be presented is the development and comparative study of different control strategies for implementation in field oriented and/or direct torque controllers for the BDFRM. In addition to the maximum power factor, being the focus of the investigation, the other control properties to be looked at allow efficiency improvement of the machine and include the maximum torque per inverter ampere and the minimum copper losses. Issues related to the influence of the pole-numbers and functionality of the windings on the machine efficiency shall be also addressed in an attempt to answer which winding should be grid-connected and which inverter-fed so that the total copper losses are minimised.

2. PERFORMANCE CONSIDERATIONS

This section is concerned with the derivation and analysis of expressions for an ideal BDFRM (i.e. no magnetic saturation and iron losses) which are suitable for control purposes. Neglecting the saturation effects and assuming a constant magnetising inductance in the machine model are valid approximations due to the primary winding grid-connection, and the fact that the machine is virtually fully fluxed under all loading conditions. The corresponding inductance variations are consequently too small to affect the model accuracy significantly. The consideration of iron losses (especially in the rotor) and the development of appropriate models for their adequate representation is extremely difficult for this particular machine and is out of scope of this paper. Some attempts have been recently made in this direction, and a realistic model for the BDFRM proposed based on preliminary electromagnetic analyses [25]. However, the validity of this model has not been experimentally verified.

The starting point, in the following discussion, are the space-vector equations for the BDFRM in rotating reference frames [7, 20, 21]:

$$\underline{v}_p = R_p \underline{i}_p + \frac{d\underline{\lambda}_p}{dt} + j\omega\underline{\lambda}_p \qquad (1)$$

$$\underline{v}_s = R_s \underline{i}_s + \frac{d\underline{\lambda}_s}{dt} + j(\omega_r - \omega)\underline{\lambda}_s \tag{2}$$

$$\underline{\lambda}_p = L_p \underline{i}_p + L_{ps} \underline{i}^*_{sp} \tag{3}$$

$$\underline{\lambda}_s = L_s \underline{i}_s + L_{ps} \underline{i}^*_{ps} \tag{4}$$

where subscripts `*p*' and `*s*' denote the primary and secondary windings, $L_{p,s,ps}$ are the constant three phase inductances of the windings (see Appendix inductances), $\omega_r = \omega_p + \omega_s$ is the rotor `electrical' velocity (rad/s) and $\omega_{p,s}$ are the winding applied frequencies (rad/s). It can be shown [7, 20, 21] that the machine produces usable torque if $\omega_r = p_r \omega_{rm} = \omega_p + \omega_s$ where the number of rotor poles is $p_r = p + q$ and p and q $(p \neq q)$ are the windings pole-pairs (Fig. 1). The same velocity relationship holds true for the BDFM's ancestor - the cascaded induction machine [26].

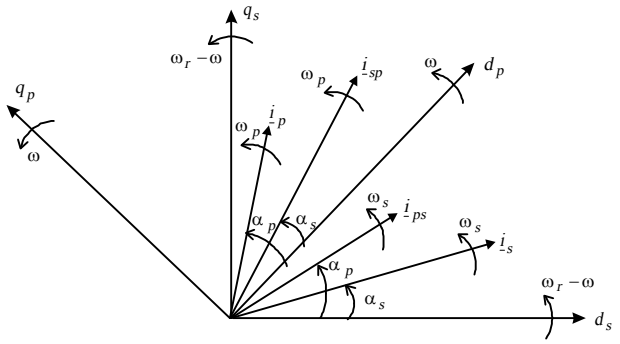

Fig. 2. The reference frames and current angle definitions for the BDFRM

Several important remarks can be made about -:

- The primary and secondary equations are in two different reference frames, rotating at ω and $\omega_r - \omega$ respectively (Fig. 2), because $\omega_p \neq \omega_s$. It is interesting that, except for this double frame referencing, the equations are nearly identical in form to DEWRIM's, despite the fundamentally different operating principle. Therefore, similar control algorithms can be used for both the machines [22, 27].
- The $\underline{i}^*_{sp}$ and $\underline{i}^*_{ps}$ terms in and are the complex conjugates of the `coupled' current vectors from the secondary to the primary winding side and vice versa and rotate at ω_p and ω_s relative to a stationary frame respectively (Fig. 2). In other words, they represent the $\underline{i}_{s,p}$ vectors referred to their complementary winding side but in a frequency (not turns ratio) sense. This frequency transformation is a consequence of the rotor's modulating influence on the stator mmf waveforms which is the basic principle behind electromechanical energy conversion in the BDFRM [21].
- As $\underline{i}_{sp} = \underline{i}_s$ in their respective frames (Fig. 2) the $d_p q_p$ components of $\underline{i}^*_{sp}$ (and hence the secondary to primary flux coupling term $L_{ps} \underline{i}^*_{sp}$) can be effectively controlled by the secondary $d_s q_s$ currents. This forms the basis of field oriented control for this machine, since one only needs to know the secondary frame position [16].

The above equations can be significantly simplified (especially the primary ones) by choosing the generic reference frame $d_p q_p$ to be aligned with the primary flux vector ($\underline{\lambda}_p$). This is a natural choice as the grid-connected (primary) winding is of fixed line frequency and approximately constant flux magnitude (as $R_p i_p << \omega_p \lambda_p$). Doing so, causes and to be with respect to the $\omega = \omega_p$ frame, while and are in the $\omega_r - \omega_p = \omega_s$ frame. The constant flux and frame alignment conditions immediately follow from and can be expressed as:

$$\lambda_p = L_p i_{pd} + L_{ps} i_{sd} + j(\underbrace{L_p i_{pq} - L_{ps} i_{sq}}_{=0}) \tag{5}$$

Using the general expression for complex power input -- $P_{3\phi} + jQ_{3\phi} = \frac{3}{2}(\underline{v}_p \underline{i}_p^* + \underline{v}_s \underline{i}_s^*)$, and substituting for -, one can derive the *vector control form expressions* for various performance measures for the machine in terms of the secondary currents (directly controllable via the inverter) and the electromagnetic torque which normally appears as an output of a speed control loop. Using motoring convention, the respective equations are as follows:

$$P_{p_{3\phi}} = P_{cu_p} + P_p = \frac{3}{2} R_p i_p^2 + \frac{\omega_p}{p_r} T_e \tag{6}$$

$$P_{s_{3\phi}} = P_{cu_s} + P_s = \frac{3}{2} R_s i_s^2 + \frac{\omega_s}{p_r} T_e \tag{7}$$

$$T_e = \frac{P_p + P_s}{\omega_{rm}} = p_r \frac{P_p + P_s}{\omega_p + \omega_s} = \frac{3}{2} p_r \frac{L_{ps}}{L_p} \lambda_p i_{sq} \tag{8}$$

$$Q_p = \frac{3}{2} \frac{\omega_p \lambda_p}{L_p} (\lambda_p - L_{ps} i_{sd}) \tag{9}$$

$$Q_s = \frac{3}{2} \omega_s \frac{L_{ps}}{L_p} \left[\left(\frac{1}{k_{ps}^2} - 1 \right) L_{ps} i_s^2 + \lambda_p i_{sd} \right] \tag{10}$$

$$i_p = \frac{\lambda_p \sin \alpha_s}{L_p \sin(\alpha_p + \alpha_s)}; \qquad i_s = \frac{\lambda_p \sin \alpha_p}{L_{ps} \sin(\alpha_p + \alpha_s)} \tag{11}$$

$$\begin{aligned} P_{cu} = P_{cu_p} + P_{cu_s} &= \frac{3}{2} \frac{R_p}{L_p^2} \lambda_p^2 + \frac{3}{2} \left(R_p \frac{L_{ps}^2}{L_p^2} + R_s \right) i_{sq}^2 \\ &+ \frac{3}{2} \left(R_p \frac{L_{ps}^2}{L_p^2} + R_s \right) i_{sd}^2 - 3 \frac{R_p}{L_p^2} \lambda_p L_{ps} i_{sd} \end{aligned} \tag{12}$$

where p_r is the number of rotor poles, $k_{ps} = L_{ps} / \sqrt{L_p L_s}$ is the coupling coefficient between the windings and $\alpha_{p,s}$ are the primary and secondary current angles (Fig. 2). The latter are mutually dependent so that is always satisfied. The relationship between these angles in a normalised form can be found in Table tb:table of the Appendix normalisations.

Again, a number of important observations can be made from the above expressions (and their normalised equivalents in Table 1):

- The equation (8) shows that one can control the machine torque in an independent manner by the q -axis secondary current as $\lambda_p =$ const. Since $i_{sq} = i_s \sin\alpha_s$ (Fig. 2) the maximum torque per inverter ampere (MTPIA)[2] i.e. the minimum inverter current for a given torque is achieved if the secondary current angle is $\alpha_{s_{mtpia}} = \pi/2$. The same equation also indicates that the torque per ampere improves with increasing the L_{ps}/L_p ratio as this allows better magnetic coupling between the windings. The ratio of the effective turns per pole of the windings (n_s/n_p) should be therefore made as higher as possible as follows from (16) in Appendix inductances. It has been shown in [16] that with $n_s = n_p$, the same amount of active material and the same copper losses the BDFRM has lower MTPIA compared to an equivalent Syncrel, but is capable of reaching much higher speeds and developing more power using the same inverter. Its maximum power output per inverter ampere is consequently better than the Syncrel's.

- As we can see from (6) and (9), even though we cannot vary the machine primary flux, we are able to regulate the grid power factor in a decoupled fashion since the reactive power (Q_p) is only affected by the d -axis secondary current (i_{sd}). The unity primary power factor (UPPF) is obtained when $Q_p = 0$ and occurs at:

$$\alpha_{s_{uppf}} = \cos^{-1}\frac{\lambda_p}{L_{ps} i_s} = \tan^{-1}\frac{T_n}{2} \tag{13}$$

where T_n is the normalised torque output. From (5) and its normalised counterpart in Table 1, the corresponding primary current angle is $\alpha_{p_{uppf}} = \pi/2$ as $i_{pd_{uppf}} = 0$. This result is expected as the primary current vector in quadrature with the flux producing d_p -axis contributes no flux in the machine. The secondary winding would be carrying all of the magnetising current for the machine in this case and the inverter current rating required would consequently be higher.

- Following on from the previous remark and setting $Q_s = 0$ (i.e. $Q_{sn} = \phi_s = 0$ in the respective expressions of Table 1), it is not difficult to show that the unity secondary power factor (USPF) i.e. the lowest inverter VA for a lossless machine, can be accomplished if:[3]

$$\begin{aligned} i_{sd_{uspf}} &= -\frac{\lambda_p + \sqrt{\lambda_p^2 - 4\left(\frac{1}{k_{ps}^2}-1\right)^2 L_{ps}^2 i_{sq}^2}}{2\left(\frac{1}{k_{ps}^2}-1\right)L_{ps}} < 0 \\ \alpha_{s_{uspf}} &= \tan^{-1}\frac{-\sqrt{1 - T_n^2\left(\frac{1}{k_{ps}^2}-1\right)^2} - 1}{T_n\left(\frac{1}{k_{ps}^2}-1\right)} > \frac{\pi}{2} \end{aligned} \tag{14}$$

[2]The term `maximum torque per secondary ampere' (MTPSA) will be also interchangeably used throughout the paper for this control strategy.

[3]Note that the maximum secondary power factor angle is not $\pi/2$ i.e. the corresponding d -axis current is not zero as the control frame is primary (not secondary) flux oriented.

where i_{sq} is directly related to torque as follows from (8). The significance of good magnetic coupling between the windings is more than evident from the same equations -- the higher k_{ps} the lower reactive power (Q_{sn}) and the better power factor $(\cos\phi_s)$.

- The secondary power expression, (7), clearly indicates the slip energy recovery nature of the BDFRM's operation as the supply inverter only has to handle the amount of power proportional to $|\omega_s = -s\omega_p|$ i.e. the degree of slip s . In this respect, the BDFRM behaves as a double-fed induction machine and this characteristic is the reason that a fractionally rated inverter can be used for restricted speed changes above and below the synchronous speed $(\omega_{syn} = \omega_p / p_r)$ when s is small[4]. If the secondary was fed with the line frequency then the BDFRM would rotate at $2\omega_{syn}$ (i.e. at the speed of a conventional $2p_r$ -pole synchronous machine) and the two windings would then evenly contribute to the machine's power output $(P_p = P_s)$. Therefore, from a real power perspective the inverter obviously needs to be rated at most to handle 50% (plus losses) of the machine's real power rating. Note that the inverter will need a larger rating if some of the flux producing current is handled by the secondary.

- If $\omega_{sn} = s = 0$ then DC is being fed to the secondary and the BDFRM is operating as a classical field controlled $2p_r$ -pole synchronous turbo-machine with α_s effectively becoming the torque angle [5]. The inverter only compensates for the secondary copper losses under this condition, as follows from (7). Supplying the primary from another converter, then a brushless variable speed synchronous machine suitable for high speed field weakened applications would be realised.

- If $\omega_{sn} < 0$ (which means the opposite phase sequence to the primary) then the power being taken from the grid by the primary is passing through the machine to be returned back to the supply via the secondary, suffering losses on its way. In this inefficient `power circulating' operating region of the machine, a fully regenerative and appropriately rated inverter would be required for sustained operation. However, if this mode is only used for starting (the machine is at standstill for $s = -\omega_{sn} = 1$) then resistive dumping would be quite sufficient. A more practical, more economical, and for the inverter less stressful solution is replace the inverter with external resistors and start the BDFRM as an induction machine [16]. An alternative method would be to use the controllable inverter for starting the machine with the shorted primary windings and then self-synchronizing it to the grid for doubly-fed operation, by applying a procedure for commercial DEWRIM drives [28].

- The i_{sd} dependent component terms in (12) illustrate the possibility of controlling the amount of copper losses in the machine in much the same manner as the Q_s for a given torque output, i.e via i_{sd} . However, unlike the (Q_p) case, the control of copper losses (and Q_s) is not decoupled from torque, due to the presence of the i_{sq} component in (12). It is easy to show from (12) and its rearranged normalised form in Table tb:table that the minimum copper losses (MCL) are achieved if:

$$i_{sd_{mcl}} = \frac{\lambda_p L_{ps}}{L_{ps}^2 + \frac{R_s}{R_p} L_p^2} \Leftrightarrow \alpha_{s_{mcl}} = \tan^{-1} \frac{r_p + r_s \zeta^2}{2r_p} T_n \tag{15}$$

[4]This property makes the BDFRM an ideal brushless candidate for pump-type applications where the speed range required is typically 2:1 or less [2].

where $\zeta = L_p / L_{ps}$ (see Appendix inductances). Therefore, in order to minimise i_{sd} and hence maximise torque per inverter ampere under MCL conditions one needs to increase R_s / R_p ratio which, given (20) of Appendix 3 resistances, translates to: $n_s \geq n_p$, $A_s \leq A_p$ and $p < q$. It should be noted that the observation about the windings turns per pole relationship for improved torque per ampere performance $(n_s / n_p \geq 1)$ is consistent with that made earlier.

- Another important comment about the MCL control strategy is that, unlike all the others considered previously, it is the only one affected by the windings pole-numbers. This dependence is introduced via the stator resistances (see (12) and (15)) and it means that it does matter which winding is a power winding and which one has a control function. Issues related to this are the subject of the subsequent sections.

3. CONTROL PROPERTIES AND TRADE-OFFS

The following analysis shall assume that the BDFRM windings have the same number of effective turns per pole $(n_s = n_p)$ i.e. $L_p = L_s$ and the same gauge copper wire i.e. the same cross section $(A_s = A_p)$. It will be based on the machine's normalised expressions in Table 1 of Appendix 2 normalisations. A 6/2-pole machine with a 4-pole rotor shall be considered assuming $k_{ps} = 1/\zeta = 7/9$ (equivalent to a typical Syncrel rotor saliency ratio of 8 [6]).

3.1 Constant torque operation

Fig. 3 demonstrates the machine's ability to control primary (and secondary) power factor from leading to lagging via the secondary current angle. Notice that for $\alpha_s < \alpha_{s_{uppf}}$ ($\approx 26^\circ$ under the conditions assumed) both power factors decrease towards zero as the primary winding is generating large amounts of reactive power into the grid, this being taken by the secondary winding from the inverter. It can be seen in Fig. 4 that in order to maintain the constant flux operation of the machine in this region the α_p angle increases to counteract the flux increasing effect of decreasing α_s angles. If $\alpha_s > \alpha_{s_{uppf}}$, then the primary power factor again deteriorates but with the primary now absorbing reactive power from the mains supply to flux the machine. The secondary power factor consequently improves reaching its maximum at $\alpha_{s_{uspf}} \approx 110^\circ$ when the primary winding becomes fully responsible for the flux production and the α_p values are small as shown in Fig. 4.

The impact of secondary current angle variations and winding pole-numbers on the machine's copper losses can be understood from Fig. 5. It can be seen that for the $p > q$ pole-pair combination (dashed curve) the MCL current angle is smaller than in $p < q$ case (solid line) indicating a higher d -axis secondary current (i_{sdn}) and inverter current loading in the first case. This means that the torque per ampere is better under $p < q$ condition which conforms with the remark made earlier. At lower α_s angles both curves show a sharp increase of losses due to dominant secondary currents. The losses, as expected, are higher when $p < q$ since $R_s > R_p$ and $i_p << i_s$. The situation is quite opposite at larger α_s values and small i_s, when the primary winding losses predominate. This trend is also evident from the third (dashed-dotted) characteristic in the same figure.

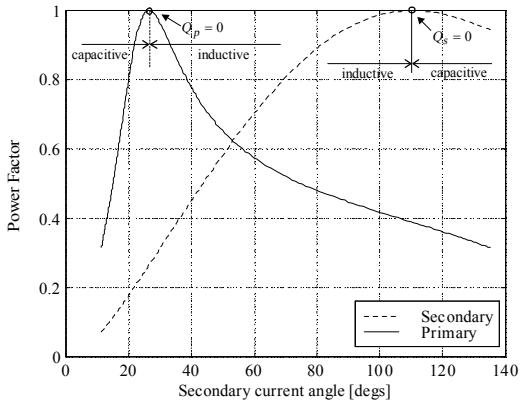

Fig. 3. Winding power factors for $T_n = 1$.

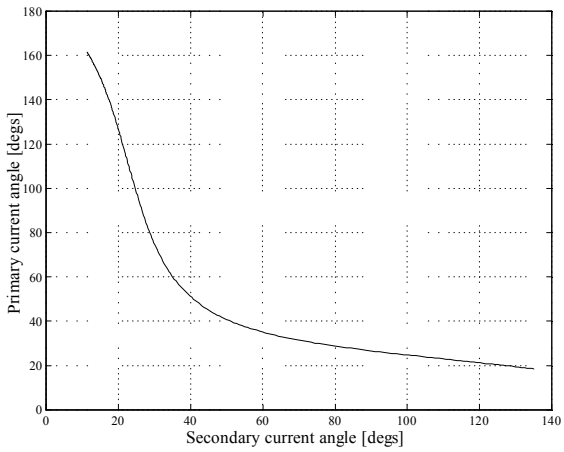

Fig. 4. Current angle relationship at $T_n = 1$

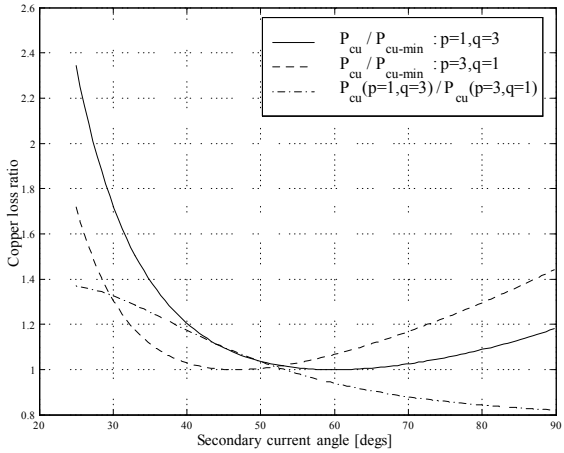

Fig. 5. Effects of winding pole-number combinations on copper losses at 1-pu torque

3.2 Optimal control aspects at various torque levels

The plots of (13), (14) and (15), for maximum power factor and minimum copper loss strategies implemented in a torque controller, are presented in Fig. 6. The fact that the USPF secondary current has a demagnetising effect (as $\alpha_{s_{uspf}} > \pi/2$ i.e. $i_{sd_{uspf}} < 0$) means that a significant extra d -axis current is needed in the primary to preserve constant flux in the machine. As a result, the USPF i_{pn} is about 2.5 its UPPF value (Fig. 7) at 1-pu torque, the ratio being even higher at lower torques when most of the USPF current is flux

producing (note the virtually flat curve in this torque range) and the UPPF current (a coupled i_{sqn} as $\alpha_{p_{uppf}} = \pi/2$ and $i_{pdn} = 0$) is small. Note from Fig. 6 that the UPPF angles are the smallest of all as the secondary current is then entirely responsible for the machine magnetization and its d -axis component is at its largest.

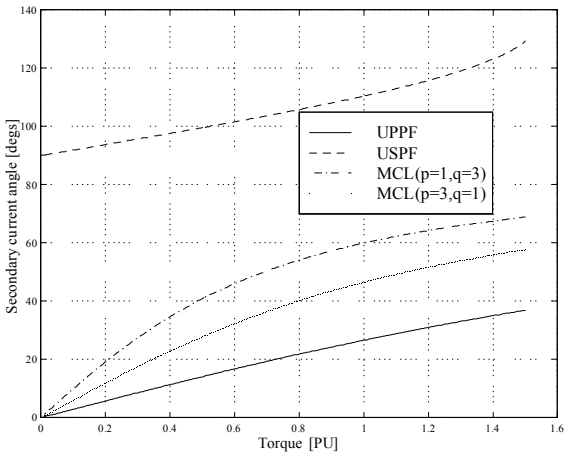

Fig. 6. Optimal control angles at various torque levels

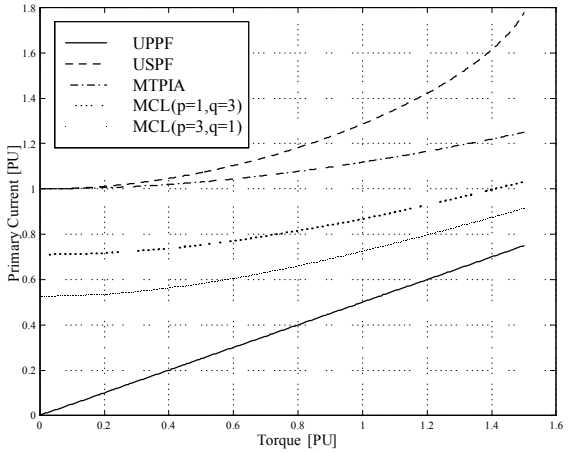

Fig. 7. Primary winding currents under optimal conditions

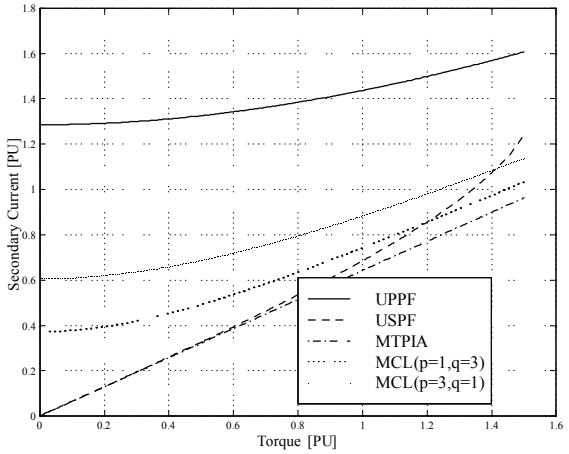

Fig. 8. Secondary winding currents for considered control methodologies

From Fig. 6 one can also notice the higher values for the minimum copper loss (MCL) angles at any torque when $p < q$. This indicates the lower secondary current magnitudes (at least 20%) compared to the $p > q$ case as shown in Fig. 8. Therefore, as far as the

torque per inverter ampere strategy is concerned, the use of a high pole winding for control purposes is a preferable option as a smaller inverter is then needed.

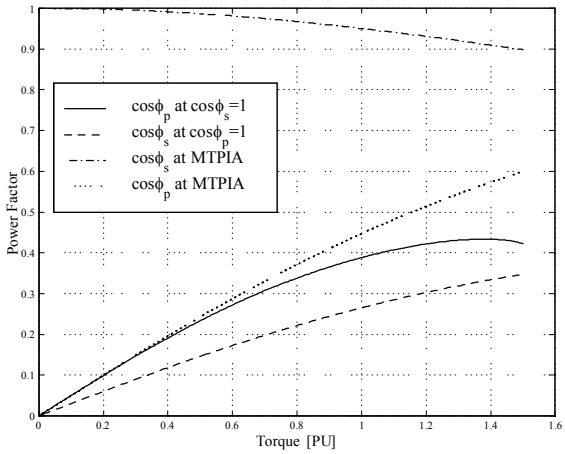

Fig. 9. Power factors for different control strategies

Along the line of the previous discussion, it would be interesting to see what influence power factor control has on the inverter size required for a BDFRM drive system. If the UPPF is desired, then the values of α_s are low and the secondary power factor is poor (Figs. 3 and 9) indicating an inefficient use of the inverter, the current rating of which would have to be higher for a given torque as illustrated by the top characteristic in Fig. 8.

The situation is diametrically opposite under the USPF conditions when the α_s angles are above $\pi/2$ and the secondary carries less reactive current. One can see in Fig. 8 that $i_{sn_{uspf}} \approx 0.5 i_{sn_{uppf}}$ at $T_n = 1$ (and less at lower torque values) meaning that at least a half rated inverter can be used in this case. However, the primary power factor is then a compromise and its maximum value is 0.4 approximately (Fig. 9).

For the reasons indicated above, similarly to the DEWRIM [19], a line-side bridge (PWM rectifier) of the bi-directional supply converter can be used for the primary reactive power (and DC link voltage) regulation, and the machine-side bridge for control of torque and secondary reactive power. In either case, one needs to trade off the size (rating) of one bridge with the other. It has been shown, however, that optimally designed radially-laminated reluctance rotors, as opposed to the axially-laminated counterparts, can offer a significant overall performance improvement to the BDFRM (including the power factor increase) to the extend that it can compete favorably with the DEWRIM of similar frame size [13]. Note that the performance enhancement considered in [13] has been achieved with machine design parameters and under conditions (which are impossible to represent analytically) different to those assumed in this paper.

If the machine is operated at the maximum torque per secondary ampere (MTPSA), the primary power factor can be slightly improved (Fig. 9) relative to the USPF value and the inverter current rating further reduced (Fig. 8) but at the cost of moving away from the optimum inverter VA i.e. USPF point (Fig. 9).

The inverter current loading under MCL conditions for $p < q$ is quite close to an optimum, but only around unity or higher pu torques (Fig. 8). The corresponding primary power factor is better than the MTPSA value but is still very low (less than 0.6 at 1-pu torque) as illustrated in Fig. 10. As expected, the secondary power factor is compromised relative to the MTPSA strategy (especially at lower torques) its value being 0.7 at unity torque as compared to approximately 0.95 under MTPSA conditions.

Another important aspect of this analysis is to examine the impact of the two pole-number combinations of the windings on the power factor performance of the machine with minimum copper losses. From Fig. 10 it is evident that the secondary power factor increases with torque for $p < q$ (dashed curve), as opposed to $p > q$ (dashed-dotted line). This results from the greater α_s angles and lower magnetising currents of the secondary winding in the first case (Fig. 6). The situation is opposite for primary power factor, due to the counteracting effect of the primary current angles required to maintain constant flux operation of the machine. This means that α_p decreases as α_s angles increase as shown in Fig. 4. As a consequence, for a primary power factor control strategy a multi-pole power winding and a 2-pole control winding is a better solution.

From a viewpoint of minimum copper losses in the machine, the $p < q$ case appears to allow lower losses in the torque range up to about 0.95-pu according to Fig. 11. At higher torque values, $p > q$ seems to be more efficient. The differences in losses are more pronounced at very low torques (less than 10%), and hence the overall efficiency may be affected more significantly, as it has a tendency to decrease at small output powers. At mid range and higher torques, however, these variations are minor (only a few percent), and their impact on the machine efficiency is virtually negligible. Therefore, with respect to efficiency, unless the machine is to be used at low powers relative to its rating, it is irrelevant which winding is grid connected and which is inverter fed.

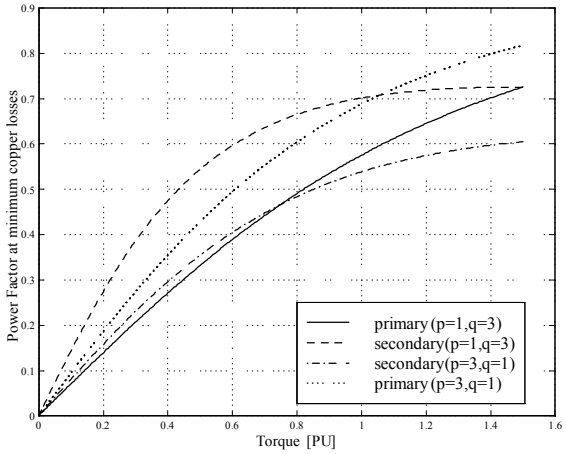

Fig. 10. Power factor performance with minimum copper losses

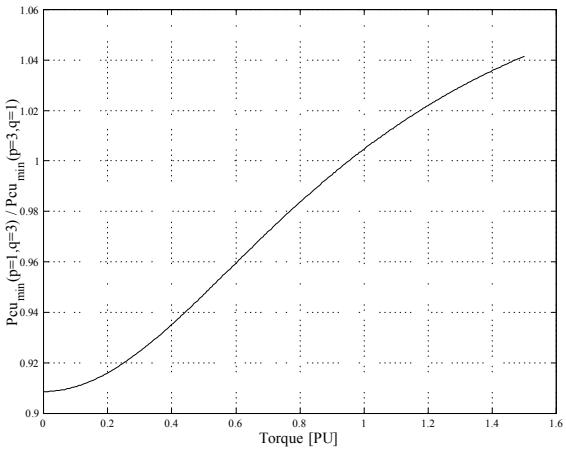

Fig. 11. Influence of winding pole-numbers on minimum copper losses

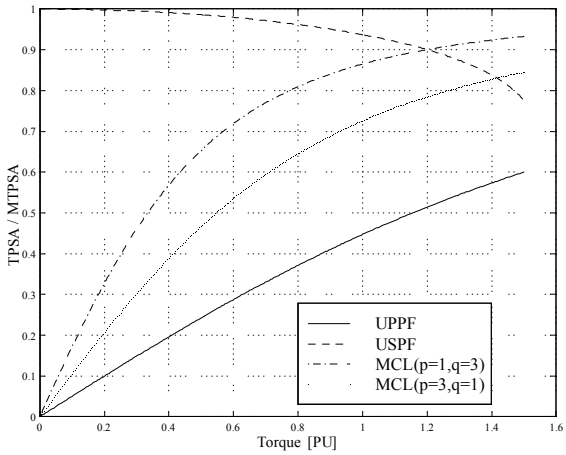

Fig. 12. Torque per secondary ampere at optimum power factors and minimum copper losses

The final part of this paper is a comparative study of the control strategies in terms of torque per secondary ampere (TPSA) performance. The plots in Fig. 12 represent the TPSA normalised to the optimum MTPSA value (corresponding to $\alpha_s = \pi/2$) . The results in this figure fully match those in Fig. 8. After MTPSA strategy, the TPSA is the highest under USPF conditions, and it is the lowest at UPPF, when the inverter current loading is a maximum (as follows from Fig. 8). Fig. 12 yet again confirms the previously made conjecture of TPSA values being higher in the case of a machine with 2-pole primary and 6-pole secondary windings and minimum copper losses.

4. CONCLUSION

This paper has performed a comprehensive comparative analysis of the BDFRM's control properties and has developed a set of useful expressions suitable for implementation of various optimal control strategies for the machine. Aspects of power factor regulation and effects of winding pole-numbers on the machine performance have been particularly emphasised. The main conclusions/observations that can be made from the presented results are:

- The inverter current rating would have to be increased approximately twice for unity primary power factor (UPPF) control at the same torque output, as compared to the other strategies considered.
- Under the UPPF conditions the secondary power factor is less than 0.3, indicating at least three times greater inverter kVA requirement for a given power output of a lossless machine. At the unity secondary power factor (USPF) and the minimum inverter kVA, the primary power factor is barely 0.4 .
- The maximum torque per secondary ampere and the USPF operating characteristics are quite close, especially at lower torques where they virtually coincide.
- All the performance parameters (except for the primary power factor), under minimum copper losses conditions, generally improve with a two-pole power winding (grid connected primary) and a multi-pole control winding (inverter-fed secondary). The primary power factor is better for the opposite situation (i.e. $p > q$) .
- The above optimum pole-pair relationship $(p < q)$ allows lower copper losses and higher efficiency in the normal torque range, and particularly at smaller torque values.

The paper has provided a valuable insight into the operation and optimal control of the BDFRM and can serve as a good reference for the interested readers wishing to initiate research in this direction. The consideration of the machine performance/inverter rating trade-offs is important as in the long run the success or failure of this interesting and unusual machine will be likely decided by whether the compromise between a larger machine for a given output torque, and a smaller size of the inverter, lead to a lower system cost in the target applications.

APPENDIX 1

Inductance Definitions

The BDFRM's inductance[5] relationships listed below have been developed using the method of winding functions [20] with the air-gap parameters as in Fig. 13. The expressions derived are, however, more general than those in [20] as they assume the nonzero permeance i.e. finite air-gap width along the rotor q -axis.

$$\left.\begin{aligned}
\text{Primary: } L_p &= \tfrac{3}{2}\mu_0 n_p^2 m\pi rl + L_{l_p} \\
\text{Secondary: } L_s &= \tfrac{3}{2}\mu_0 n_s^2 m\pi rl + L_{l_s} \\
\text{Mutual: } L_{ps} &= \tfrac{3}{4}\mu_0 n_p n_s n\pi rl \\
\zeta &= \tfrac{L_p}{L_{ps}} \approx \tfrac{n_p}{n_s}\tfrac{2m}{n} \\
m &= y\Lambda_d + (1-y)\Lambda_q \\
n &= \tfrac{2}{\pi}(\Lambda_d - \Lambda_q)\sin\pi y
\end{aligned}\right\}$$

where:

$n_{p,\,s}$ ≙ effective turns/pole/phase of the windings

$L_{l_{p,\,s}}$ ≙ leakage inductances of the windings

$r,\ \ l$ ≙ machine mean radius and axial length

$1/\Lambda_d$ ≙ minimum air-gap width

$1/\Lambda_q$ ≙ maximum air-gap width

y ≙ pole-arc/pole-pitch ratio of the rotor (Fig. 13)

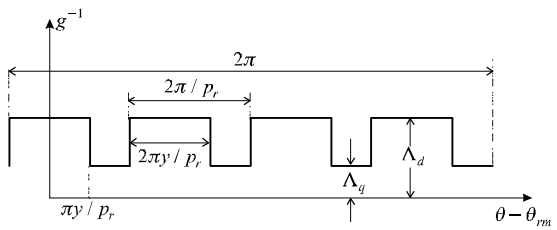

Fig. 13. Inverse air-gap function for a 4-pole reluctance rotor used for inductance determination (θ , some mechanical angle around the stator circumference; θ_{rm} , the mechanical angle of the rotor high permeance axis)

[5]In practice, the actual inductance values can be identified from measurements by applying the off-line testing methods presented in [14].

Table 1 :Normalized control from expressions and base quantities

Primary quantities
$i_{pn} = \frac{\sin\alpha_s}{\sin(\alpha_p+\alpha_s)} = \frac{\sqrt{(2\tan\alpha_s - T_n)^2 + T_n^2\tan^2\alpha_s}}{2\tan\alpha_s}$
$\left.\begin{array}{l}\lambda_{pn} = i_{pdn} + \frac{1}{\zeta} i_{sdn} = 1 \\ i_{pqn} - \frac{1}{\zeta} i_{sqn} = 0\end{array}\right\} \Leftrightarrow \tan\alpha_p = \frac{T_n\tan\alpha_s}{2\tan\alpha_s - T_n}$
$P_{pn} = \frac{1}{2}T_n; \quad Q_{pn} = 1 - \frac{i_{sdn}}{\zeta} = 1 - \frac{T_n}{2\tan\alpha_s}$
$\cos\phi_p = \frac{P_{pn}}{\sqrt{P_{pn}^2+Q_{pn}^2}} = \frac{T_n\tan\alpha_s}{\sqrt{(T_n^2+4)\tan^2\alpha_s - 4T_n\tan\alpha_s + T_n^2}}$
Secondary quantities
$i_{sn} = \frac{\zeta\sin\alpha_p}{\sin(\alpha_p+\alpha_s)} = \frac{\zeta T_n\sqrt{1+\tan^2\alpha_s}}{2\tan\alpha_s}$
$P_{sn} = \frac{\omega_{sn}}{2}T_n = \omega_{sn}P_{pn} = -sP_{pn}$
$Q_{sn} = \frac{\omega_{sn}T_n}{4\tan^2\alpha_s}\left[T_n\left(\frac{1}{k_{ps}^2}-1\right)(\tan^2\alpha_s+1) + 2\tan\alpha_s\right]$
$\phi_s = \tan^{-1}\frac{Q_{sn}}{P_{sn}} = \tan^{-1}\frac{T_n(1/k_{ps}^2-1)(\tan^2\alpha_s+1)+2\tan\alpha_s}{2\tan^2\alpha_s}$
Torque, power output and copper losses
$T_n = \frac{2}{\zeta} i_{sqn} = \frac{2}{\zeta} i_{sn}\sin\alpha_s$
$P_n = P_{pn} + P_{sn} = \frac{1+\omega_{sn}}{2}T_n = \omega_{rn}T_n$
$P_{cun} = \frac{4r_p\tan\alpha_s(\tan\alpha_s - T_n) + T_n^2\left(r_p + r_s\zeta^2\right)\left(\tan^2\alpha_s+1\right)}{4\tan^2\alpha_s}$
$P_{cun_{\min}} = P_{cun}(\alpha_{s_{mcl}}) = \frac{\left(r_p+r_s\zeta^2\right)^2 T_n^2 + 4r_p r_s\zeta^2}{4\left(r_p+r_s\zeta^2\right)}$
Base values
Torque & power : $T_B = \frac{3}{4}p_r\frac{\lambda_p^2}{L_p} \quad P_B = \frac{2\omega_p T_B}{p_r}$
Current & flux : $i_B = \lambda_B / L_p \quad \lambda_B = v_B / \omega_p$

APPENDIX 2

Normalisations

In order to make machine performance expressions independent of its parameters a set of normalisations corresponding to the arbitrary chosen $\alpha_p = \alpha_s = \pi/4$ condition has been developed taking the grid voltage and frequency as bases (see Table 1).

APPENDIX 3

Stator resistance expression

Consider a single full-pitch turn of a generic P -pole sinusoidally distributed winding. The total length and resistance of the turn are:-

$$l_t = \text{length in slots} + \text{end turn length} = 2l + \frac{2\pi d}{P}$$

$$R_t = \frac{\rho_{cu} l_t}{A} = \frac{2\rho_{cu}}{A}(l + \frac{\pi d}{P}) = \frac{2\rho_{cu} d}{A}(\beta + \frac{\pi}{P})$$

where:

$l \triangleq$ length of the machine stack

$d \triangleq$ diameter from the centre of the stator slots

$\rho_{cu} \triangleq$ resistivity of conductive material (copper)

$A \triangleq$ cross-sectional area of the wire used

$\beta = l/d \triangleq$ machine's aspect ratio

If the winding has n effective turns per pole and phase then its total phase resistance is:-

$$R = P \cdot nR_t = \frac{2\rho_{cu} d}{A} n(P\beta + \pi)$$

Applying this to the BDFRM windings and assuming $\beta \approx 0.5$ for convenience (a NEMA180 frame), then the resistances of the $2q$ -pole secondary and $2p$ -pole primary winding can be related as follows:-

$$\frac{R_s}{R_p} = \frac{n_s}{n_p} \cdot \frac{A_p}{A_s} \cdot \frac{q + \pi}{p + \pi}$$

REFERENCES

[1] Y. Liao, Design of a brushless doubly-fed induction motor for adjustable speed drive applications, *Proceedings of the IAS Annual Meeting*, pp. 850–855, San Diego, California, October 1996.

[2] B. Gorti, D. Zhou, R. Spée, G. Alexander, and A. Wallace, Development of a brushless doubly-fed machine for a limited speed pump drive in a waste water treatment plant, *Proc. of the IEEE-IAS Annual Meeting*, pp. 523–529, Denver, Colorado, October 1994.

[3] M. G. Jovanovic, R. E. Betz, and J. Yu, The use of doubly fed reluctance machines for large pumps and wind turbines, *IEEE Transactions on Industry Applications*, vol. 38, pp. 1508–1516, Nov/Dec 2002.

[4] L. Xu and Y. Tang, A novel wind-power generating system using field orientation controlled doubly-excited brushless reluctance machine, *Proc. of the IEEE IAS Annual Meeting*, Houston, Texas, October 1992.

[5] O. Ojo and Z. Wu, Synchronous operation of a dual-winding reluctance generator, *IEEE Transactions on Energy Conversion*, vol. 12, pp. 357–362, December 1997.

[6] R. E. Betz and M. G. Jovanovic, The brushless doubly fed reluctance machine and the synchronous reluctance machine - a comparison, *IEEE Transactions on Industry Applications*, vol. 36, pp. 1103–1110, July/August 2000.

[7] R. E. Betz and M. G. Jovanovic, Introduction to the space vector modelling of the brushless doubly-fed reluctance machine, *Electric Power Components and Systems*, vol. 31, pp. 729–755, August 2003.

[8] P. Bauer, S. de Haan, C. R.Meyl, and J. T. G. Pierik, Evaluation of electrical systems for off-shore windfarms, *IAS Annual Meeting*, Rome,Italy,2000.

[9] F. Saifkhani and A. K. Wallace, A linear brushless doubly-fed machine drive for traction applications, *Proc. of the European Power Electronics Conference*, pp. 344–348, Brighton,UK,September 1993.

[10] A. K. Wallace, R. Spee, and G. C. Alexander, Adjustable speed drive and variable speed generation systems with reduced power converter requirements, *Proc. of the International Symposium on Industrial Electronics (ISIE)*, pp. 503–508, 1993.

[11] S. Williamson, A. Ferreira, and A. Wallace, Generalised theory of the brushless doubly-fed machine. part 1: Analysis, *IEE Proc.-Electric Power Applications*, vol. 144, pp. 111–122, March 1997.

[12] L. Xu and F. Wang, Comparative study of magnetic coupling for a doubly fed brushless machine with reluctance and cage rotors, *IEEEIAS Annual Meeting*, pp. 326–332, New Orleans, Louisiana,October 1997.

[13] E. M. Schulz and R. E. Betz, Optimal torque per amp for brushless doubly fed reluctance machines, *CD-ROM Proc. of IEEE-IAS Annual Meeting*, Hong Kong, October 2005.

[14] F. Wang, F. Zhang, and L. Xu, Parameter and performance comparison of doubly-fed brushless machine with cage and reluctance rotors, *IEEE Transactions on Industry Applications*, vol. 38, pp. 1237–1243, Sept/Oct 2002.

[15] D. Zhou, R. Spee, and G. C. Alexander, Experimental evaluation of a rotor flux oriented control algorithm for brushless doubly-fed machines, *IEEE Transactions on Power Electronics*, vol. 12, pp. 72–78, January 1997.

[16] L. Xu, L. Zhen, and E. Kim, Field-orientation control of a doubly excited brushless reluctance machine, *IEEE Transactions on Industry Applications*, vol. 34, pp. 148–155, Jan/Feb 1998.

[17] R. Li, R. Spee, A. K. Wallace, and G. C. Alexander, Synchronous drive performance of brushless doubly-fed motors, *IEEE Transactions on Industry Applications*, vol. 30, pp. 963–970, July/August 1994.

[18] L. Xu, Analysis of a doubly-excited brushless reluctance machine by finite element method, *Proceedings of the IEEE IAS Annual Meeting*, pp. 171–177, 1992.

[19] R. Pena, J. C. Clare, and G. M. Asher, Doubly fed induction generator using back-to-back PWM converters and its application to variable-speed wind-energy generation, *IEE Proc. - Electr. Power Appl.*, vol. 143, pp. 231–241, May 1996.

[20] F. Liang, L. Xu, and T. Lipo, D-q analysis of a variable speed doubly AC excited reluctance motor, *Electric Machines and Power Systems*, vol. 19, pp. 125–138, March 1991.

[21] Y. Liao, L. Xu, and L. Zhen, Design of a doubly-fed reluctance motor for adjustable speed drives, *IEEE Transactions on Industry Applications*, vol. 32, pp. 1195–1203, Sept/Oct 1996.

[22] Y. Liao and C. Sun, A novel position sensorless control scheme for doubly fed reluctance motor drives, *IEEE Transactions on Industry Applications*, vol. 30, pp. 1210–1218, Sept/Oct 1994.

[23] M. G. Jovanovic, J. Yu, and E. Levi, Direct torque control of brushless doubly fed reluctance machines, *Electric Power Components and Systems*, vol. 32, pp. 941–958, October 2004.

[24] M. G. Jovanovic, J. Yu, and E. Levi, Encoderless direct torque controller for limited speed range applications of brushless doubly fed reluctance motors, *IEEE Transactions on Industry Applications*, vol. 42, pp. 712–722, May/June 2006.

[25] I. Scian, D. G. Dorrell, and P. J. Holik, Assessment of losses in a brushless doubly-fed reluctance machine, *IEEE Transactions on Magnetics*, vol. 42, pp. 3425–3427, October 2006.

[26] B. Hopfensperger, D. J. Atkinson, and R. A. Lakin, Stator flux oriented control of a cascaded doubly-fed induction machine, *IEE Proc. - Electr. Power Appl.*, vol. 146, pp. 597–605, November 1999.

[27] L. Xu and W. Cheng, Torque and reactive power control of a doubly fed induction machine by position sensorless scheme, *IEEE Transactions on Industry Applications*, vol. 31, pp. 636–642, May/June 1995.

[28] L. Morel, H. Godfroid, A. Mirzaian, and J. M. Kauffmann, Double-fed induction machine: Converter optimisation and field oriented control without position sensor, *IEE Proc. - Electr. Power Appl.*, vol. 145, pp. 360–368, July 1998.